

PETROS EIKON INCORPORATED
222 Snidercroft Road, Concord, Ontario
Canada, L4K 2K1

**Coal Authority Phase 2:
Theoretical Modelling Study**

R.W. Groom
April 28, 2004

Contents:

1. Introduction	2
2. Background	2
3. Methodology	2
4. Reciprocity of Measurement System	3
5. Shaft Reciprocity	4
6. Tomograms	5
7. Results	6
8. Analyses and Recommendations	8
9. Conclusion	9
10. References	9
11. Figures	9

1. Introduction

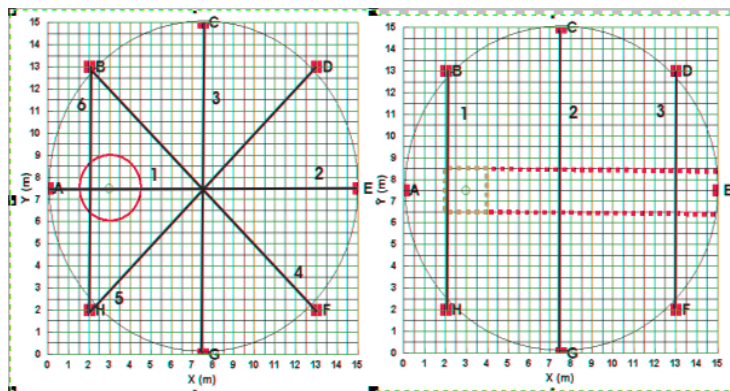
This report describes a theoretical modelling project to study the effectiveness of a crossborehole Radio Imaging Method (RIM) to locate and image mineshafts and adits. One simple model of a borehole shaft containing three different materials (air, water and backfill) in a uniform 2-layer background was utilized and one model of an adit (air filled) was used in the same background material. A series of boreholes were utilized all having a length of 30m and all boreholes are perfectly normal to a flat earth surface.

2. Background:

For this geophysical RIM data system, the transmitter (Tx) and receiver (Rx) antennae are both 1.5m in length and are Reciprocal@ or identical in nature. They consist of a flexible center tube with wire wound around the tube but no magnetic material is contained within the windings. Typically the diameter of the windings are from 1.8in to 3in depending on the application. Since the number of windings are relatively small with no internal magnetic material, the TX transmits electric field but not magnetic field effectively and the Rx picks up electric fields effectively but is not sensitive to magnetic fields. Therefore, for this study only the radiated electric fields as detected theoretically by the antennae were utilized.

A data Apanel@ consists of placing the Tx at a set of depths in one hole and the Rx=s at a set of depths in the another distant hole. Data is collected at the Rx locations for each Tx location. Receivers are positioned at 1m intervals in one borehole and transmitters at 1m intervals in the other borehole. Both Tx and Rx positioning began centered at depths of 2m to account for antennae length and the cover thickness of 1m. Rx/Rx locations end at a depth of 29m to account for hole length and antennae length. This distribution is common for all boreholes. All models were run at 4 frequencies: 100,300,600, 900KHz. The normal operating frequency of the actual system ranges between 100-990KHz range. The 4 sample frequencies covered the principle variations with frequency.

3. Methodology



8 borehole locations were utilized (Figure 1) labelled A-H. 6 different borehole geometries (panels) were used in the shaft study and are labelled 1-6 on the left side of Figure 1. 3 panels (1-3) were used for the adit study and are shown on the right of Figure 1.

For each panel and for each borehole, 28 1.5m length electrical antennae were placed at 1m intervals in each borehole of a panel. Due to the length of the antennae, the first antennae was placed with its centre at 2m depth so as not to cross into the overlying cover and the last antennae was placed with its centre at 29m so as to fit in the borehole (depth 30m). At each Tx, 4 frequencies in the AM radio band (100,300,600&900KHz) were radiated and both the background signal and the secondary signal from either the shaft or the adit was calculated at each Rx in the opposite borehole. Thus, 28x28 simulated measurements were made for each panel at each frequency.

The numerical technique utilized for the forward modelling (electric field simulation) is an integral equation technique termed the Localized Nonlinear Approximator (Habashy, Groom, Spies, 1993). The integral equation technique involves first calculating the response due to the layered background. This calculation provides the background response at the Rx=s but also the incident fields which excite the 3D target to generate secondary or scattered fields. The integral equation technique utilizes the incident fields to calculate equivalent sources inside the 3D target. These equivalent sources then radiate the secondary fields (in this case the electric fields) to be picked up by the receivers. The shaft target was discretized to 3x3x60 points (sample points) at which the equivalent sources are determined. A numerical integration is then performed over the equivalent sources to generate the secondary fields. The Tx=s and Rx=s are represented as extended antennae (ungrounded in this case). Integration is performed over the extended Tx=s and Rx= to generate the electric fields sensed at the Rx=s. As the system proposed for the actual surveying does not at this time measure the phase of the measured electric fields, all data is shown as amplitude only.

The resulting data is displayed in several forms. Examples are seen in the report of the response at the receivers for individual Tx=s as line plots. Data panels are shown via a number of ray trace methods. The ray trace method involves determining the ray path between receiver and transmitter and weighting in the ray trace grid the amplitude contribution for each cell. Amplitudes for each cell are summed for each ray and normalized by the number of rays passing through the ray trace grid cell. Data may be either total, secondary or secondary/background normalized. As there is a geometric fall-off to the fields, a geometric renormalization is sometimes performed. A tomographic algorithm can also be performed. However, since the response to the targets (shaft,adit) do not show simple absorption this is not often performed.

4 Reciprocity of the Measurement System

The antennae are fully reciprocal in that both Rx and Tx are identical in nature and can be interchanged.. We therefore begin by illustrating the impact of reciprocity from several angles to explain the impacts of this physical situation. As an example, the response or panel for the borehole pair AE and the reciprocal pair EA are the same for the host background (ie. cover plus host material). To illustrate this Figure 2 shows the amplitude response (red) for a Tx at a depth

of 17m in Hole E and the entire set of Rx=s in Hole A and the reverse response (blue) for a Tx at the same depth in Hole A and the entire set of Rx=s in Hole E. The system as yet only measures amplitude and does not yet deliver the phase of the signal.

For Figure 2, a frequency of 600KHz is utilized.

Here (Figure 3), we view the model geometry for TX=s in hole E and Rx=s in hole A. The shaft is square and 3m on each side. The modelling algorithm is fully 3D, so that an infinite shaft cannot be used. However, by repeated modelling, it was determined that a shaft length of more than 60m showed no difference in model results from the 60m shaft and as such a 60m shaft was used for all the models. The shaft begins at a depth of 1m and continues to a depth of 61m.

Figure 4 displays the responses in Hole E due to 2 transmitters in Hole A for a water filled shaft. The plot compares the background amplitude response (blue, brown) and total response (red, green) for Tx=s namely at a depth of 21m (blue, red) and at a depth of 12m (brown, green). It is clearly seen that the shaft although causing a significant response mimics a different background material. The response with the shaft is transmitter depth independent and follows a similar geometric fall-off as the response of the background (ie. no shaft present). This, is due to the shaft being essentially infinite in length and merely acting on the system primarily as a modification in the background. Variations do occur near the top of the holes due to interactions between the cover layer and the shaft. The response shown here is for 600KHz.

This character of the response to the A infinite@ shaft and the reciprocity of the antennae lead to some unexpected results and a problem as it relates to target resolution. Figure 5 indicates the response of the air-filled shaft to the AE section (red) and the EA section (green) for a Tx in both instances at a depth of 16m at 600Khz. As can be seen from the figures, the responses are virtually identical except for the Rx at a depth of 2m from the surface. This is a numerical artifact coming from the internal gridding of the shaft. When, the Tx is moved to a deeper depth then this artifact becomes smaller and smaller and is virtually unidentifiable.

5 Shaft Reciprocity

Now, the most important issue as it relates to resolution of the shaft. Figure 5 displays what is somewhat obvious from physical principals that if the shaft is centered at x=3 then the radiation pattern of the signal from Tx to Rx is reciprocal between AE and EA panels. Now, it would also seem relatively obvious that if the shaft were moved to x=12m then the AE panel would be identical to the EA panel for a shaft at x=3m. For in this case, the Tx=s and Rx=s are reversed across the panel and the shaft is an equal distance from the Tx=s and the Rx=s in both panels. To summarize, let us call the AE panel with the shaft at x=3m, AE_forward and similarly the EA panel with the shaft at x=3, EA_forward. The AE panel with the shaft at x=12 is then termed AE_reversed. Thus, EA_forward = AE_forward due to antennae reciprocity and AE_reversed = EA_forward due to antennae reciprocity and the basic physics of Maxwell=s equations. Thus, AE_reversed = AE_forward and the response for the panel when the shaft is flipped to the other side of the panel should be identical.

Figure 6 represents this case. For a Tx depth of 16m at a water-filled shaft, the AE_forward case (ie. AE panel with shaft in correct location) is shown in red for 900Khz, EA_forward is shown in blue (squares) and AE_reversed is shown in green (thick line, crosses). Note, AE_reversed and EA_forward are identical as they are performing identical simulations (ie. rx=s and tx=s are the same distance from the shaft in both cases) but we know from reciprocity the EA_forward should equal AE_forward. Thus, although there are slight differences it is simply numerical.

The important conclusion is that the system cannot physically distinguish a shaft at $x=3$ from a shaft at $x=12$. In this case, we did not utilize a cover as there are different interactions with the cover which do give some resolution which will be seen later. Without actually knowing the background material and the geometry of the shaft in and out of the crosshole panel then from basic physical principles the shaft cannot be resolved. This is a fundamental limitation to this geophysical system for this problem.

6 Tomograms

A grid is implemented for the ray tracing and tomography algorithms. For these panels, the normal grid utilized is 27 cells in depth and 15 cells across (15m hole-to-hole separation). In other cases, the grid is double to 54x30 cells. To illustrate the techniques, we first utilize a somewhat smaller shaft to indicate that for non-infinite objects, the shaft can be detected. In this case, we utilize a 20m shaft centered at 15m depth. Figure 7 is a simple amplitude contour of Rx position vs Tx position for the entire panel for the water filled shaft. A frequency of 600Khz is utilized for this figure. It can be seen for straight crossrays (ie. Tx depth equals Rx depth), the amplitude is decreased when within the shaft depths and increased outside.

Figure 8 illustrates a simple ray trace of the secondary data. The shaft can be seen highlighted on the left side with a weaker mirror (from reciprocity) on the other side. We now impose on the data a geometric weighting (Figure 9). Knowing the position of Tx and Rx=s as well as the geometric fall-off of the antennae system, we can apply an inverse geometric fall-off weighting which shows the position of the shaft. The image is slightly asymmetrical due to the effect of the cover and air layer above. Finally, we apply a tomographic algorithm (Figure 10) which now illuminates the shaft more clearly but too close to the hole A. This is because we do not have rays that pass freely through the open area between the hole and the shaft to the other borehole.

In Figure 11, we increase the grid size by grid cells only of 0.5m in size and now we can see the eastern edge of the shaft around $x=1.5$ m which is the edge of the shaft. The actual position of the shaft is outlined in white.

These figures indicate the type of tomographic processing as well as the resolvability of finite shafts. But now we must process the actual shafts.

However, this is the end of the good news for panels AE and EA as Figure 5 has implied and Figure 6 shows.

7 Results

Figure 12 shows a comparison of responses to the 3 shaft models for a Tx in hole A at 15m depth and at 600KHz. Purple indicates the response in the absence of the shaft (background), red(air), blue(water) and green (backfill). The water shaft has a significant response and the air a somewhat weaker response. The air also has a broader response but again the response mimics very closely the background response. The response of the backfill is very weak Figure 13 is a similar plot but with a Tx depth of 24m and the propagating frequency set at 900KHz. The air has a somewhat weaker response than at the low frequency and in fact 100KHz is usually the optimum frequency for imaging the air-filled shaft. Again the air has a broader response.

7a AE, EA Panels

Air Filled: Figures 14 shows the background-reduced data for the air-filled shaft at 100Khz for panel AE. 100KHz has the largest response for the air-filled shaft. Figure 15 is for the EA panel. Note that the shaft is virtually unseen except immediately at the top where it appears for both panels. Figures 16 and 17 show the same panels but with the data geometrically reduced. The shaft is equally weakly identified in both cases.

Water Filled: Figures 18 shows the geometrically processed secondary field for the AE panel at 900Khz. 600KHz and 900KHz have virtually the same response for the water-filled shaft and are virtually identical. Figure 19 shows the geometrically processed panel for EA. The ray-traced panels are virtually identical as would be expected from reciprocity. The location of the shaft to the left of the panel is all that can be seen.

Backfill: Figure 20 shows the total field vs the background (without shaft) for 300KHz for 2 Tx's. One Tx is at the top of Hole A (Brown: Background, Green: Total Field) and the other at the bottom of Hole A (Blue: Background, Red: Total). It can be seen that there is virtually no response to the backfill at the bottom of the hole and a small response at the top. Figures 21 and 22 show ray trace panels for AE (Fig 21) and EA (Fig 22) for 300 KHz . As indicated by Figure 20, only the top of the shaft is identified due to the interactions with the top layer. The data here is processed normalized (ie. Secondary/Background)

7b Panel BF:

Figures 23 and 24 show the response comparisons for the 3 fills of the shaft (Air: Red, Water: Orange, Backfill: Green, Background: Blue). Figure 23 shows comparisons for the bottom Tx in Hole B at 100Khz (top) and 900Khz (bottom). The water filled shaft has the largest response at both high and low frequency with the other shafts having very little response but at low frequency the air has the larger of the other 2 fills and at high frequency the backfill has a larger response than the air. Figure 24 shows the same displays but for a Tx at the top of Hole B. The water filled shaft still has the largest response with air a slightly enhanced response over the background and the backfill a slightly decreased response.

Figures 25,26,27 indicate the ray trace panels of secondary/background for water, air and backfill filled shafts respectively. Slight asymmetries are seen towards the Tx hole (B) and a deepening of the response coming from the top and up from the bottom but nothing very clear except in the water filled case where the presence of something long is indicated.

7c Panel BH:

The water filled shaft has a quite different response when the holes are closer as in this case causing a distinctive flattened response in the vicinity of the transmitter. Also, the background response at lower frequencies is different that at wider separations having a crossover

Figure 28 shows the water filled shaft indicating a structure in the center. The high amplitude at the top is caused by an anomalous response near surface due to the cover interactions and the moderated high at the bottom is cause by inadequate data cover for imaging. Figure 29 shows the air-filled shaft showing the presence of a symmetric anomaly at surface and the backfill (Figure 30) shows indication but only at the top.

7d Panel CG: For panel CG, the shaft edge is 3.5m to the east of the panel and the panel is a full 15m across. Figures 31(water), Figure 32(air), Figure 33(backfill) show secondary responses at 300Khz geometrically reduced.

Line plots of the data show that there is virtually no response for the air filled or backfilled shaft except for a slight enhancement by air at the top of the panel and a slight decrease for the backfill. The water filled still has a significant response but it is almost exactly mirroring the background response (Figure 34) and thus cannot be discriminated in imaging from a different background material. There is only a weak indication of the shaft.

Figure 33 and 32 show only a slight variations at the surface symmetrically positioned which is the only indication of a target being present. The long green cross shape in the Figure 33 is characteristic of inductive fall-off not represented by the geometric fall-off indicating the inductive fall-off dominates any secondary response from the shaft . The unusual shape of Figure 33 ray trace tomograph is noteworthy. Figure 31 for the water-filled shaft shows the presence of a target symmetrically positioned.

7e Panel DH : Panel DH is a reverse panel of panel BF! This may not seem obvious but the discussion at the beginning proves this to be true. The two panels' crosshole distances are the same and the target is flipped in both symmetry planes. Since the shaft is so deep as to be considered infinite then the target is symmetric except for interactions with the surface layer. Figure 35 illustrates this showing the response for a transmitter at a depth of 11m for 900Khz for the 2 panels. There are slight differences in the panel data for transmitters near the surface particularly for the air-filled shaft but only small differences. Figure 36 can be compared to Figure 25. Figure 36 is shown in 3D to clarify the point. In this figure, borehole D (Tx=s) is to the upper

right while H is to the lower left and the shaft is closer to Hole H containing the Rx's. In Figure 25 (shown in plan view), Hole B is to the left and hole F to the right. In this case, the shaft is closer to hole B containing the Tx's. The location of the shaft is indicated by the asymmetry in the respective plots.

The air-filled shaft is difficult to image and Figure 37 is shown with different processing showing the secondary field unprocessed with the location of the shaft near hole H is indicated by three green area moved towards Hole H. Figure 38 shows the ray-tracing image for the backfilled shaft. In this case, we process the secondary field with a geometric normalization again indicating a slight asymmetric towards borehole H in the image.

7f Adit: The adit geometry was first modelled as a prism (2m x 2m) dipping to the west. It was determined that the adit had to be at least 80m in length to be represented as infinite in length. The top of the prism was then shaved off to be parallel to the cover layer and then the top placed coincident with the bottom of the cover. This model is represented for panel DF in Figure 39.

Figures 40, 41, 42 show the secondary ray trace tomogram geometrically reduced for 100KHz for Panels BH, CG and DF respectively. The location of the adit passing between the borehole pairs is rather clearly illuminated.

In addition, we also simulated the panel crossing at an angle to the adit (DH). That result is shown in Figure 43 showing the dip of the adit.

8 Analyses and Recommendations

In general, the infinite extent of the shaft and the reciprocity of the transmitter and receiver antennae do not allow distinct resolution of the shaft. The water filled shaft has a strong response but cannot be detected without knowing the background response. Reciprocity of the antennae and the shaft model leads to ambiguity in positioning for an individual panel. The air filled shaft shows a distinct interaction with the cover layer and its top is often identified. The short separation panel shows a clear indication of the shaft but its position in the center of the tomogram might be a coincidence due to the reciprocity of the model. A modified model with the shaft off-centre for the short panel (BH) might be recommended.

In general, the combination of results for all 6 panels for the shaft leads to a relative certainty with regards to its location in all but the backfill case and most strongly in the case of the water filled shaft.

Finite objects, on the other hand, are easily detected and the location of the crossing of the adit with the 3 perpendicular panels are easily seen while the dip of the adit from the non-perpendicular crossing panel is also identified. A finite shaft less in length than the boreholes is also detected.

The present system operates at sampling distance within the borehole for the Rx's at 0.2m while the sampling of the Tx is a function of survey time. It would be informative to provide models for the higher Rx sampling for those models which showed promise.

9 Conclusions

The detection of finite objects within the uniform background is easily detectable for all three types of fill given the appropriate radiating frequency. Detection of the "infinite" shafts requires some consideration as to how to properly image their location. Close panel separations for water filled shafts showed promise.

However, data sampling with the actual system is quite different than in the simulated surveys and modelling with the denser Rx sampling as obtained during actual data surveying is recommended.

In practice, however, the background material is far from uniform and the model results may be optimistic.

10 References

T. M. Habashy, R. W. Groom and B. R. Spies, *Beyond the Born and Rytov Approximations: A Nonlinear Approach to Electromagnetic Scattering*, Journal of Geophysical Research, 98, no. B2 (1993).

11 Figures

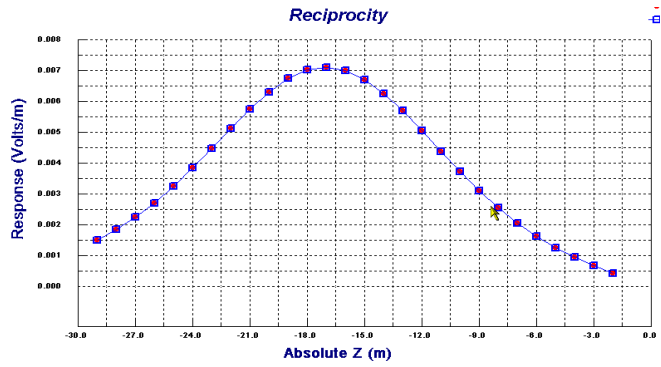


Figure 2: Reverse Antennae in Panel AE and EA

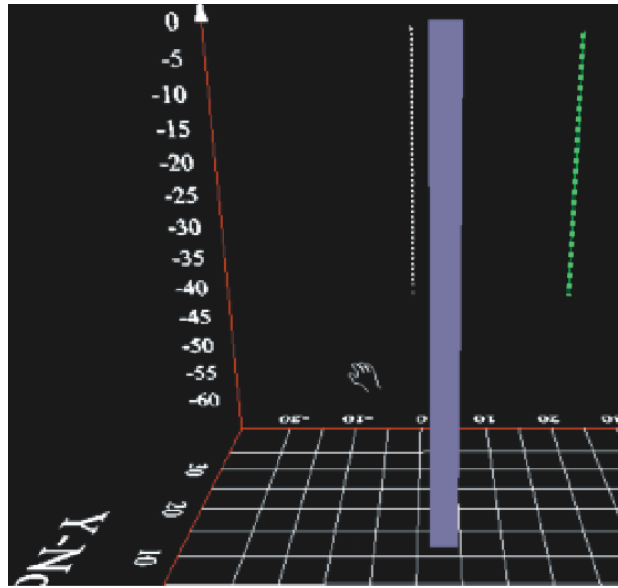


Figure 3: AE panel with 60m shaft(grey-blue)

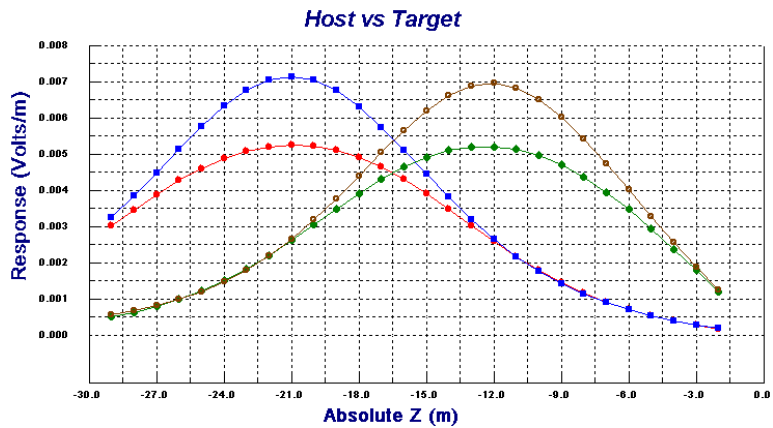


Figure 4: Response in Hole E due to Tx's in Hole A.
 Blue, Red: Tx 21m (Background, Total)
 Brown, Green: Tx 12m (Background, Total)

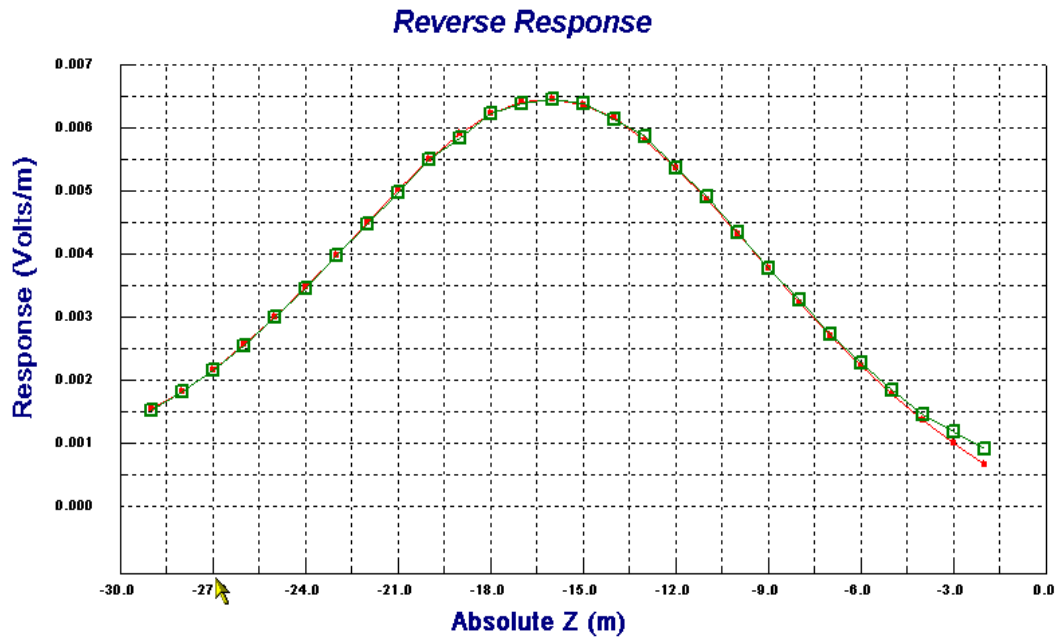


Figure 5: System Reciprocity:
A->E (red) and E->A (green), Tx at 16m

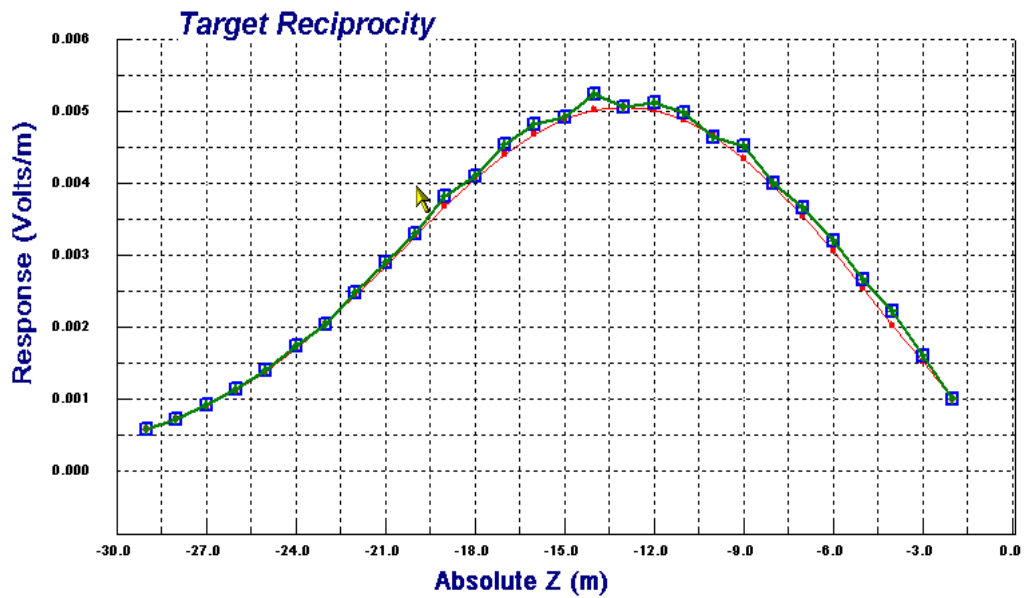


Figure 6: Target Reciprocity. Red: A->E (x=3m), Blue: E->A (x=3m), Green: A->E (x=12m)

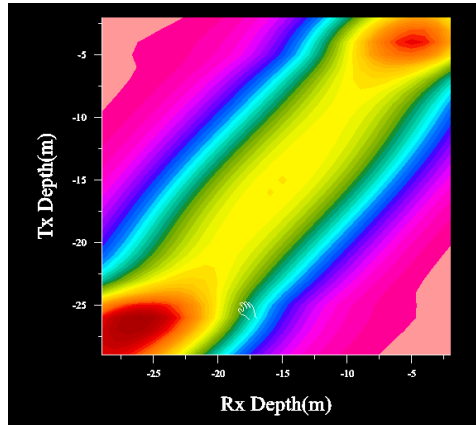


Figure 7: AE panel with 20m shaft.
600Khz.
Tx vs Rx signal amplitude. Red: High
Amplitude

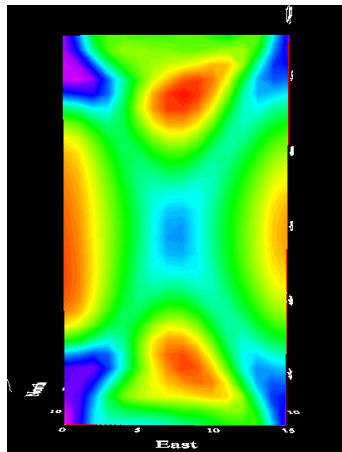


Figure 8: Secondary Data
600KHz. Red high amplitude
and Blue low.

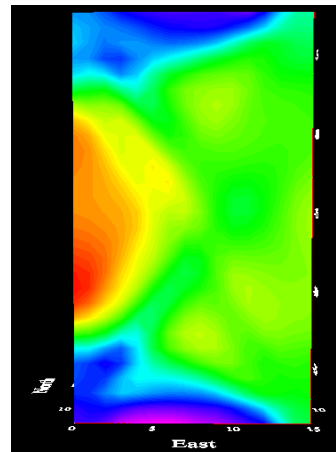


Figure 9: Secondary Data ,
600KHz
Geometric Weighting

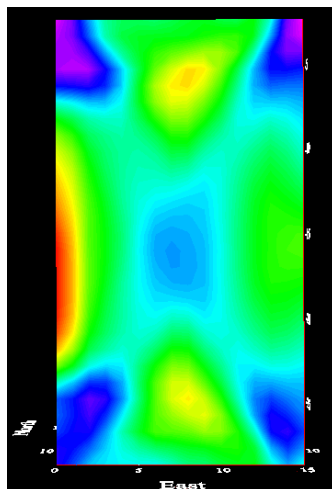


Figure 10: 1m grid:
Tomogram

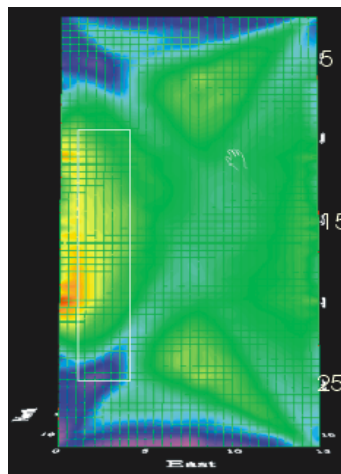


Figure 11: 0.5m Tomogram -
position of shaft is outlined in
white

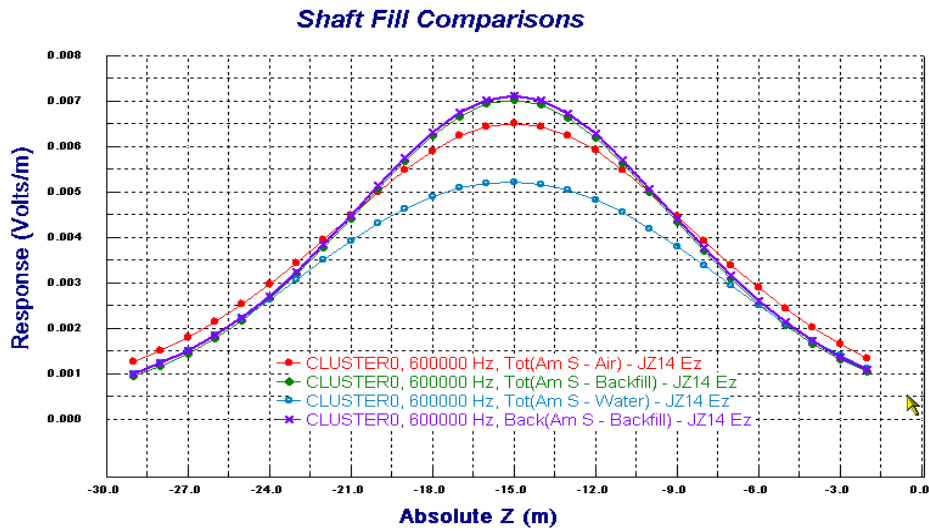


Figure 12: Shaft Fill Comparisons: Purple: background, Red: Air, Green: Backfill, Blue: Water. Tx depth 15m. 600KHz

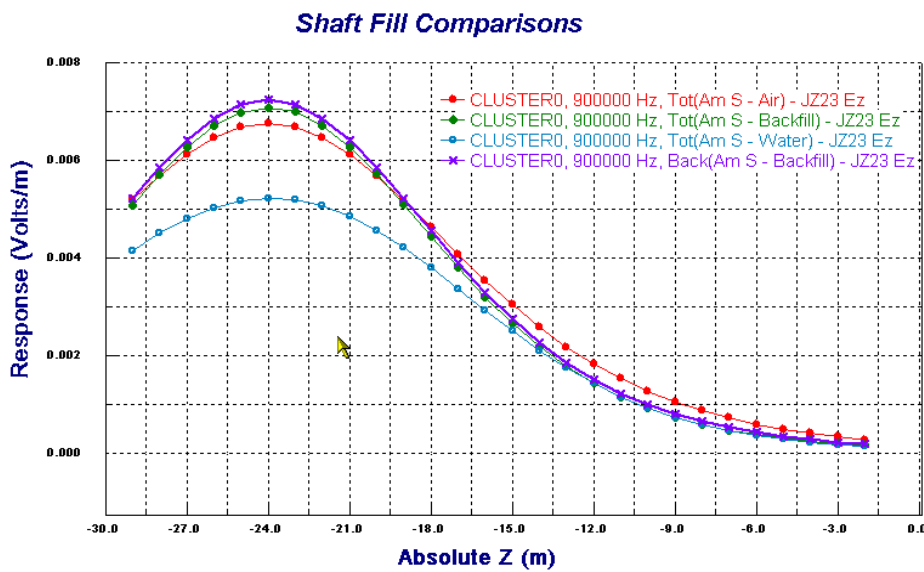


Figure 13: Shaft Fill Comparisons: Purple: background, Red: Air, Green: Backfill, Blue: Water. Tx depth 24m. 900KHz

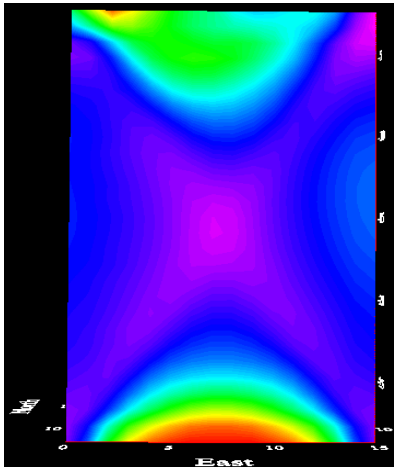


Figure 14: AE, 100Khz, Secondary Unprocessed, Air Filled

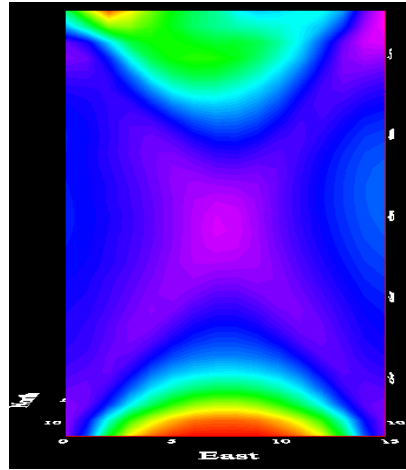


Figure 15: EA, 100Khz, Secondary Unprocessed, Air Filled

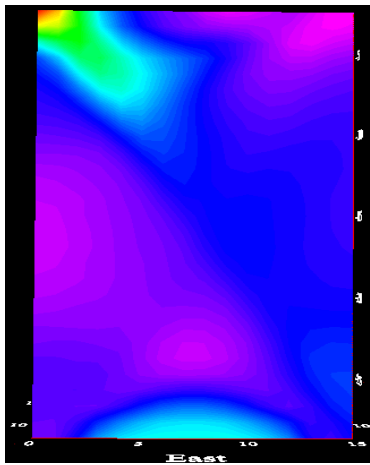


Figure 16: AE, 100Khz, Sec Geometric Processed, Air Filled

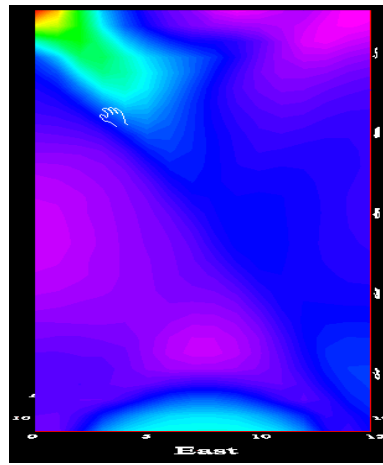


Figure 17: EA, 100Khz, Sec Geometric Processed, Air Filled

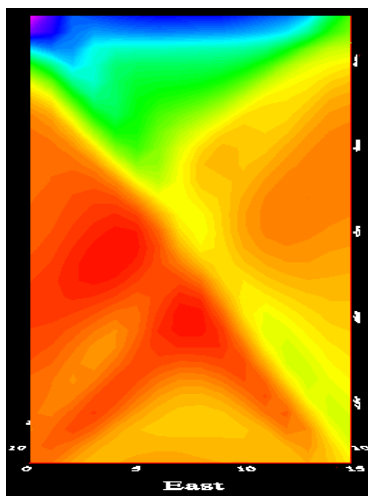


Figure 18: AE, 900Khz, Secondary Geometric Processed, Water Filled

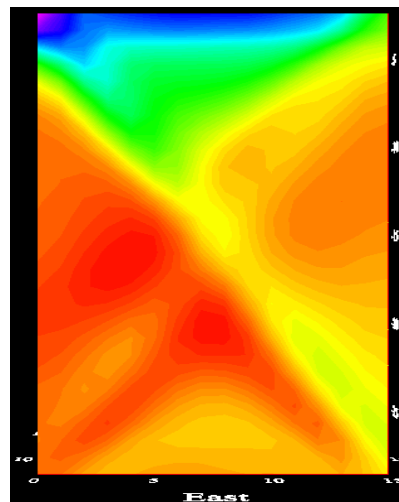


Figure 19: EA, 900Khz, Secondary Geometric Processed, Water Filled

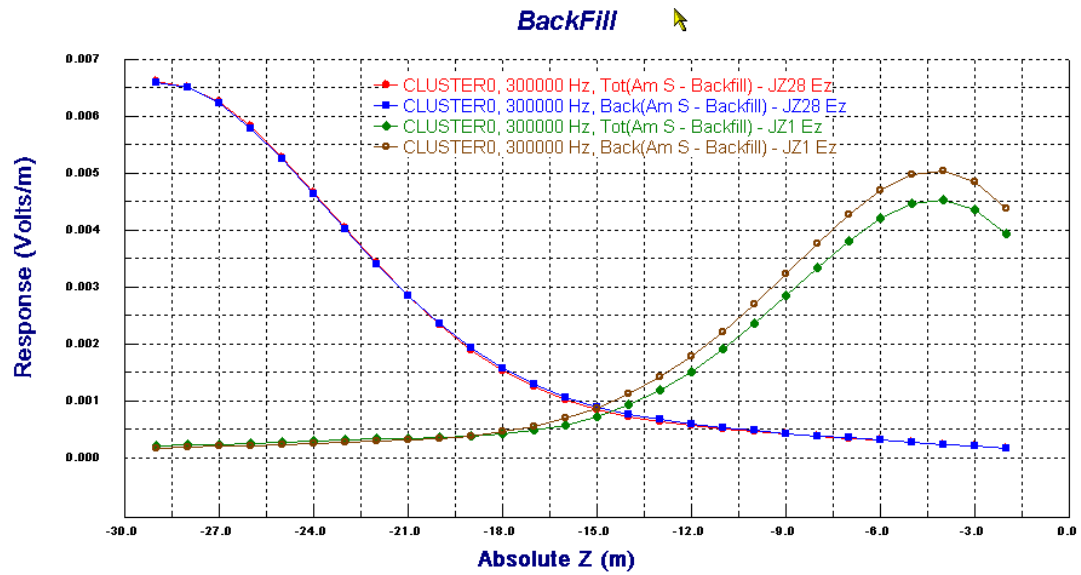
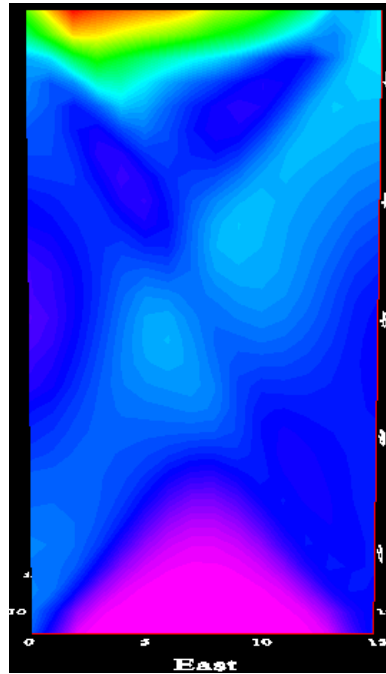
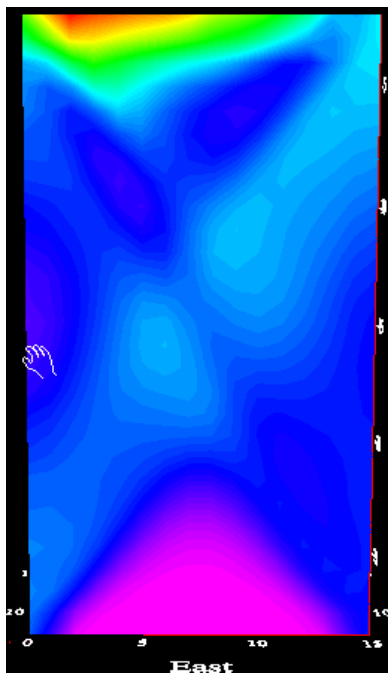


Figure 20: Backfilled Shaft: Panel AE: Total vs Background Top and Bottom Tx



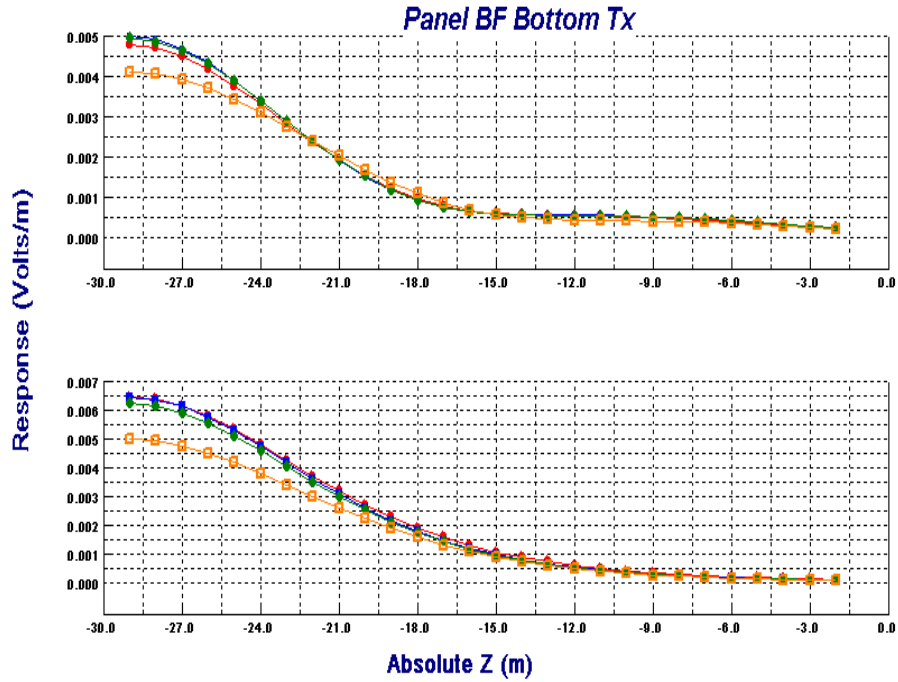


Figure 23: Panel BF Model Comparisons TX at bottom:
 Blue: Background, Orange: Water
 Green: Backfill, Red: Air. Top figure: 100KHz, Bottom figure: 900KHz

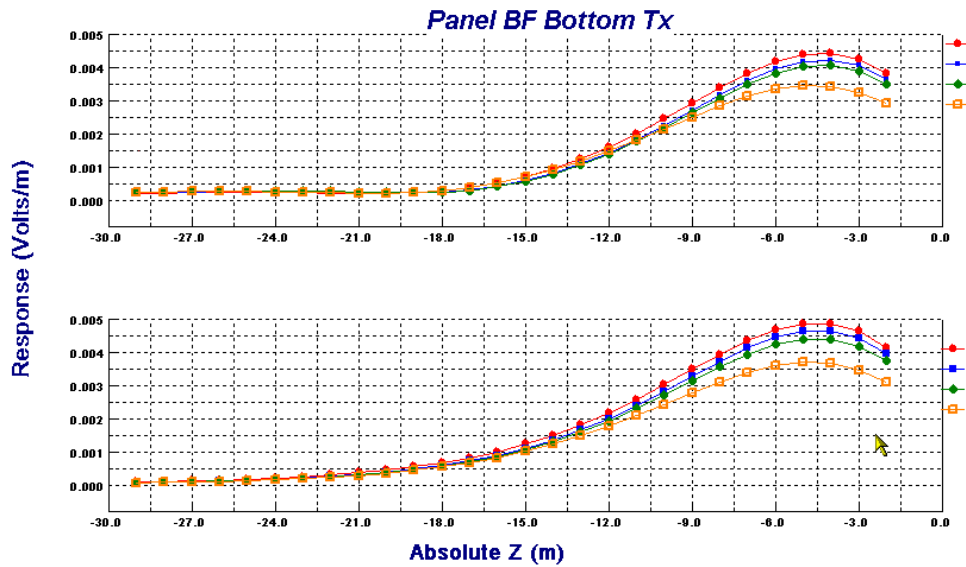


Figure 24: Panel BF Model Comparisons Tx at top
 Blue: Background, Orange: Water
 Green: Backfill, Red: Air. Top figure: 100KHz, Bottom figure: 900KHz

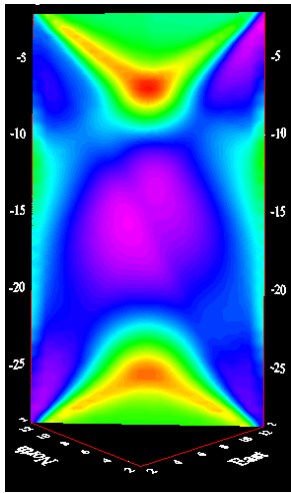


Figure 25: BF Water Filled 100KHz, Secondary/Back Hole B on left

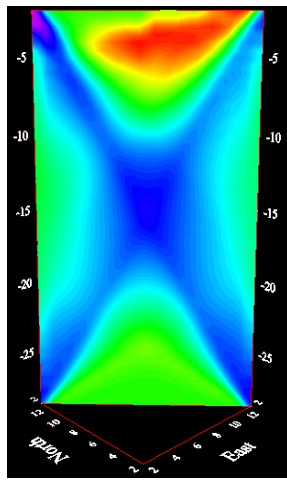


Figure 26: BF Air Filled 100KHz, Secondary/Back

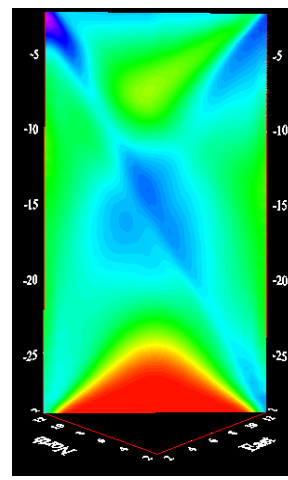


Figure 27: BF Backfill 100KHz, Secondary/Back

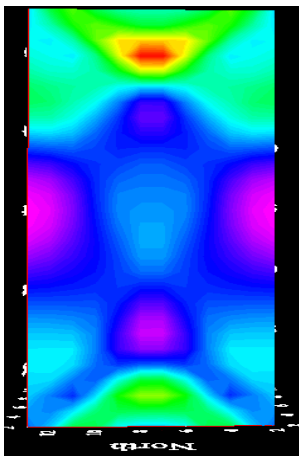


Figure 28: BH Water Filled 100KHz Secondary/Back

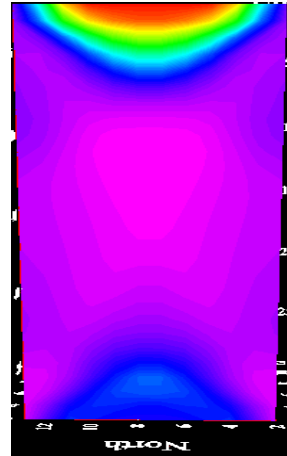


Figure 29: BH Water Filled 100KHz Secondary/Back

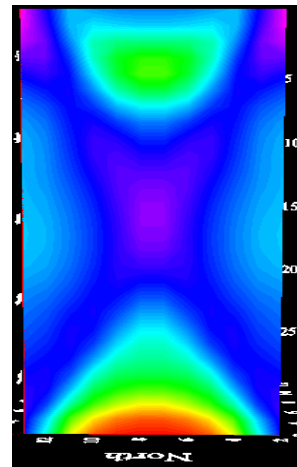


Figure 30: BH Water Filled 100KHz Secondary/Back

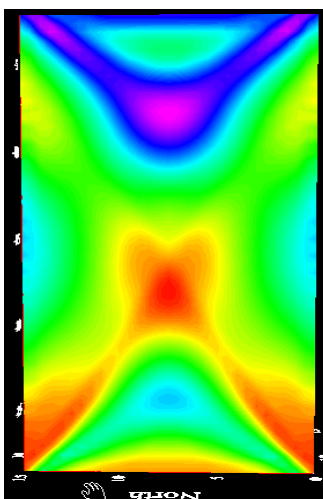


Figure 31: CG Water Filled 300KHz Secondary Reduced

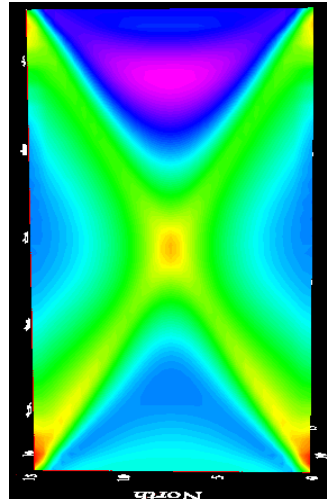


Figure 32: CG Air Filled 300KHz Secondary Reduced

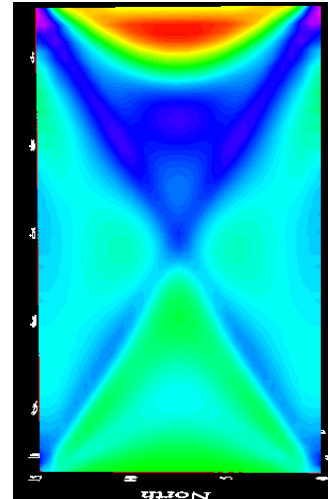


Figure 33: CG Backfill 300KHz Secondary Reduced

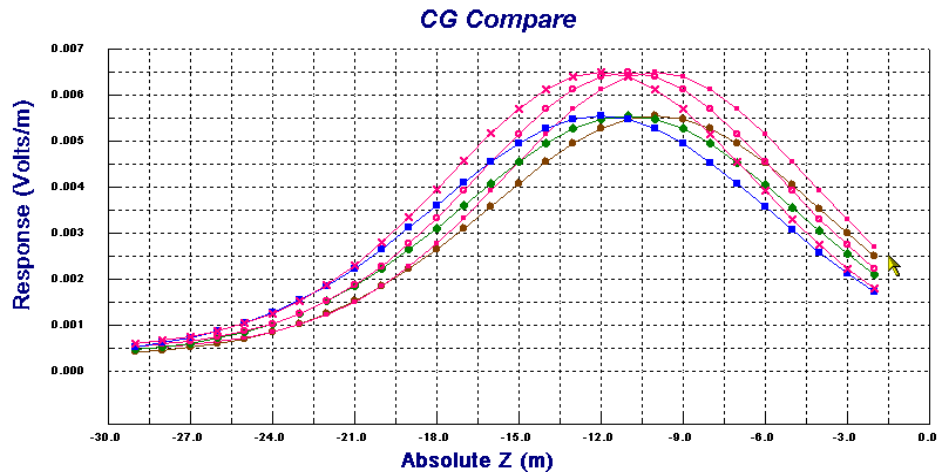


Figure 34: Background vs Waterfill: 300Khz. 3 pink curves show background at 10,11 and 12m depths. Total Field: brown(10m),green(11m),blue(12m)

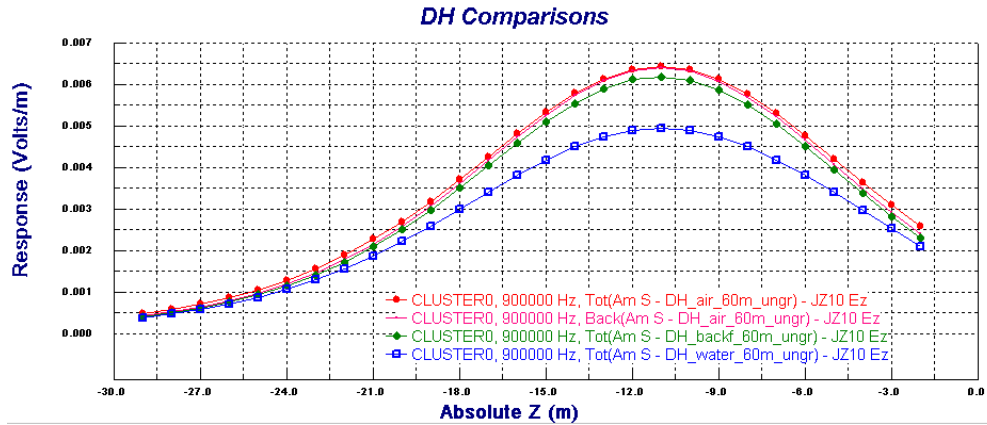


Figure 35a

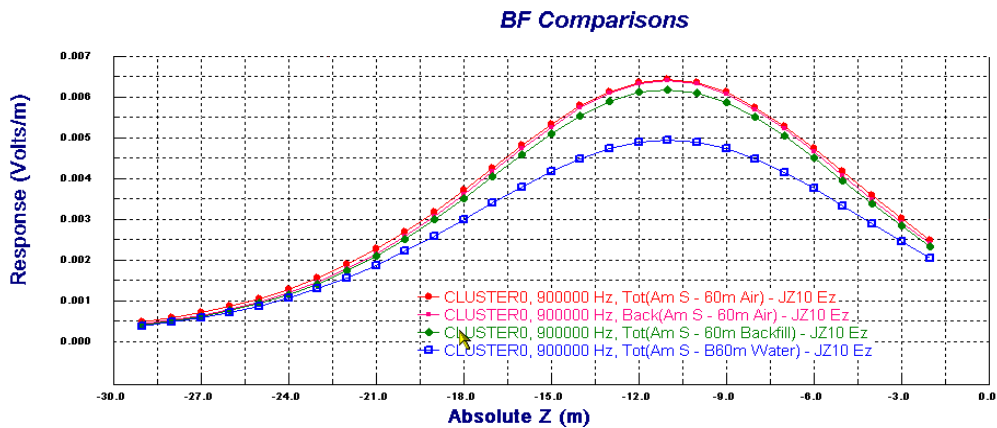


Figure 35b: Model Comparisons: DH Panel vs BF Panel: 900Khz. Tx:11m depth
 Pink: Background, Blue: Water, Red: Air, Green: Backfill
 Top (a): DH, Bottom(b): BF

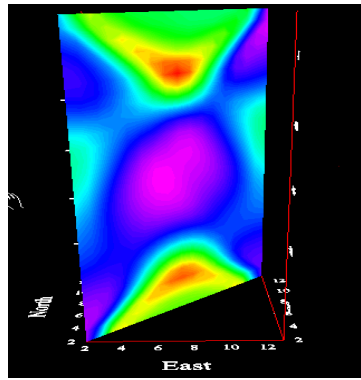


Figure 36: DH Panel: 100Khz
Water filled. Secondary/Back
Hole H: left, Hole D: right

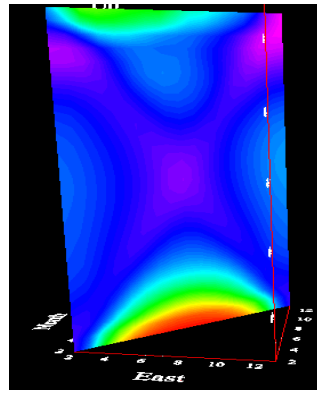


Figure 37: DH Panel:
100Khz
Air filled shaft, Secondary

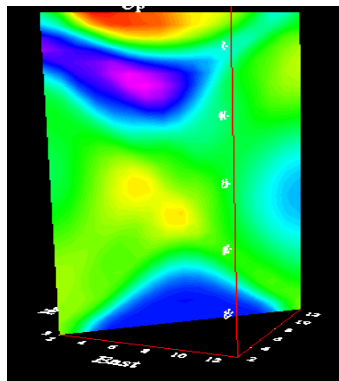


Figure 38: DH Panel: 300Khz
Backfill, Secondary
Geometric Processed

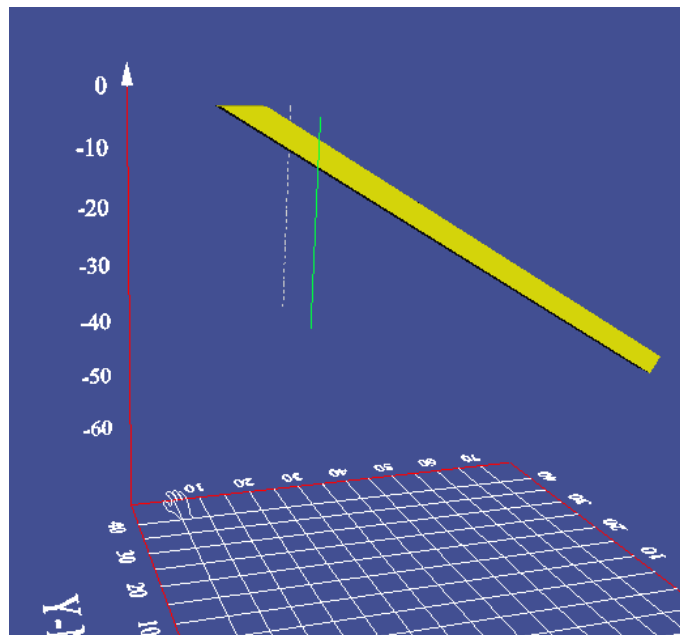


Figure 39: Adit Geometry. Panel. Hole D(grey) and H(green)

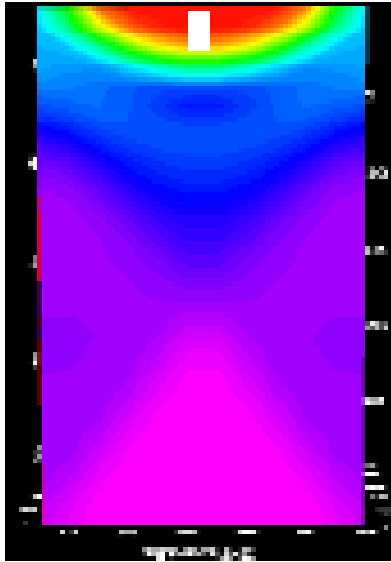


Figure 40: BH Adit, 100KHz
Secondary Geometric Proc

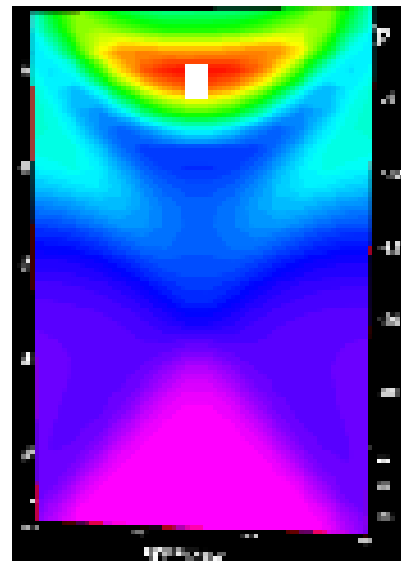


Figure 41: CG Adit, 100KHz

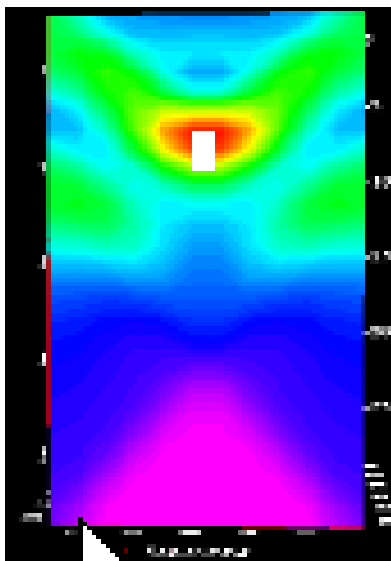


Figure 42: IF Adit, 100KHz

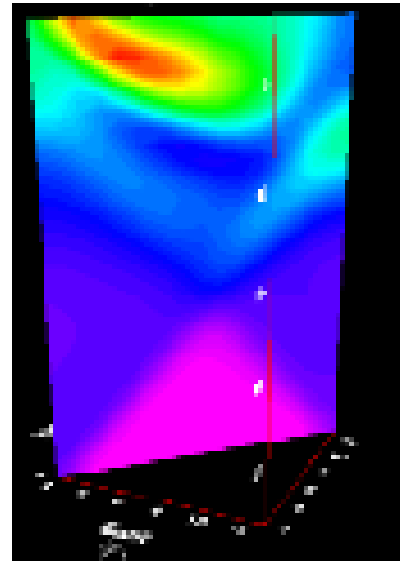


Figure 43: Adit, DM Panel